http://w3.pppl.gov/~zakharov/XL140709.pdf

Simulations of vertical disruptions with VDE code: Hiro and Evans currents

Xujing Li[1], Leonid E. Zakharov[2], Sergei Galkin[3]

[1] *Institute of Computational Mathematics and Scientific/Engineering Computing, Academy of Mathematics and Systems Science,Chinese Academy of Sciences, P.O. Box 2719, Beijing 100190, China*

[2] *Princeton Plasma Physics Laboratory, MS-27 P.O. Box 451, Princeton NJ 08543-0451*

[3] *FAR-TECH, Inc. 10350 Science Center Dr. Bld 14, St 150, San Diego, CA 92121, USA*

Theory and Simulation of Disruptions Workshop

July 09-11, 2014, PPPL, Princeton NJ

*This work is partially supported by US DoE contract No. DE-AC02-09-CH11466, and by the National Magnetic Confinement Fusion Science Program 2011GB105003

PPPL PRINCETON PLASMA PHYSICS LABORATORY

Abstract

The talk presents a recently created numerical code VDE for simulations of vertical instability in tokamaks. The numerical scheme uses the Tokamak MHD model, where the plasma inertia is replaced by the friction force, and an adaptive grid numerical scheme. The code reproduces well the surface currents generated at the plasma boundary by the instability.

Five regimes of the vertical instability are presented:

1. ***Vertical instability in a given plasma shaping field without a wall;***
2. ***The same with a wall and magnetic flux*** $\Delta\Psi|_{pl}^{X} < \Delta\Psi|_{X}^{wall}$ ***(where*** X ***corresponds to the X-point of a separatrix);***
3. ***The same with a wall and magnetic flux*** $\Delta\Psi|_{pl}^{X} > \Delta\Psi|_{X}^{wall}$***;***
4. ***Vertical instability without a wall with a tile surface at the plasma path;***
5. ***The same in the presence of a wall and a tile surface.***

The generation of negative Hiro currents along the tile surface, predicted earlier by the theory and measured on EAST in 2012, is well-reproduced by simulations. In addition, the instability generates the force-free Evans currents at the free plasma surface.

For the first time the generation of the Evans currents was reproduced by rigorous numerical simulations.

These currents being a necessary attribute of vertical instability explain the original measurements of tile currents on DIII-D in 1991, which for more than two decades misinterpreted as fictitious "halo" currents due to misuse of equilibrium reconstruction.

Contents

1 Basic equations. Macroscopic Tokamak MHD (TMHD) 4

2 VDE of a straight plasma column, CylVDE() routine 7

3 VDE on EAST 22

4 Vacuum chamber in EAST 24

5 TorVDE() for VDE simulations on EAST 25

6 VDE simulations motivate innovative diagnostics 27

7 Summary 28

Instead of hydro-dynamic "MHD of salt water" we use MHD relevant to the tokamak plasma

In general, the TMHD model utilizes the following properties of disruptions

$$\tau_{MHD} \simeq \underbrace{R/V_A}_{<1\ \mu s} \ll \underbrace{\tau_{TMHD}}_{\simeq 1\ ms} < \underbrace{\tau_{transport}}_{\simeq 0.1\ s} \ll \underbrace{\tau_{resistive}}_{\simeq 1\ s} \quad (1.1)$$

1. ***During disruptions plasma conserves magnetic fluxes. As a result, singular currents are generated at the plasma boundary and at the resonant surfaces (for $n \neq 0$)***
2. ***Plasma inertia is negligible (except along the resonant layers)***

- ***TMHD considers the disruption dynamics as a fast equilibrium evolution with conservation of magnetic fluxes and with singular currents.***
- ***At the same time TMHD provides scale separation, suitable for non-MHD physics of singular layers.***

Basic TMHD equations

1. **Equation of motion**

$$\lambda\delta\vec{r} = -\nabla p + (\vec{\jmath}\times\vec{B}) \tag{1.2}$$

No inertia, no velocity, no time, no Courant limitation on the time step

2. **Toroidal flux conservation instead of equation of state**

$$(\nabla\times(\delta\vec{r}\times\vec{B}_\varphi)) = 0. \tag{1.3}$$

3. **The resistive part of TMHD**

   (a) **Faraday's (Ohm's) law**

$$-\frac{\partial\vec{A}}{\partial t} - \nabla\varphi_E + (\vec{V}\times\vec{B}) = \frac{\vec{\jmath}^{pl}}{\sigma^{pl}}. \tag{1.4}$$

   $\vec{\jmath}$ is determined by force balance, the Faraday law determines $\vec{V}$.

   (b) **Plasma anisotropy**

$$(\vec{B}\cdot\nabla\sigma) = 0. \tag{1.5}$$

   Plasma anisotropy, $(\vec{B}\cdot\nabla T_e)\simeq 0$ is explicitly reproduced by adaptive grids

   (c) **Electro-magnetic boundary condition at a wall**

$$\vec{E}^{pl}_{\|} = \vec{E}^{wall}_{\|} = \frac{\vec{\jmath}^{pl}}{\sigma^{pl}} - (\vec{V}\times\vec{B}) = \frac{\vec{\jmath}^{wall}}{\sigma^{wall}} \tag{1.6}$$

   describes plasma shrinking.

Three step solution:

1. **Plasma core.** ***Equation of motion is split into two parts:***

$$\underbrace{\nabla p = (\vec{j} \times \vec{B})}_{GSh\ equilibrium}, \quad \underbrace{\lambda \delta \vec{r} = -\frac{\nabla \tilde{F}^2}{2r^2}}_{force\ imbalance}, \quad \left(\vec{j}_{pol} = \frac{\nabla F}{r}, \quad F \equiv \bar{F}(\bar{\Psi}) + \tilde{F}(\bar{\Psi}, \theta) \right). \qquad (1.7)$$

GSh solution is obtained first.

2. **Surface currents.** ***Matching the core magnetic field with external structures (eddy and Hiro currents in vessel, coils) leads to surface currents $\bar{\imath}$ at the plasma boundary and a pressure jump P***

$$\bar{\imath} = B_\theta^{vac} - B_\theta^{core}, \quad 2\mu_0 P \equiv B_\theta^2|_{core}^{vac} + \frac{\bar{F}^2|_{core}^{vac}}{r^2}. \qquad (1.8)$$

3. **Advancing plasma boundary.** ***Poloidal currents $\tilde{F}$ from the core make the surface currents force-free.***

Toroidal flux conservation $(\nabla \times (\delta \vec{r} \times \vec{B}_\varphi)) = 0$ is reduced to

$$\delta \vec{r} = r(\nabla U \times \mathrm{e}_\phi), \quad \left(\nabla \cdot \frac{\delta \vec{r}}{r^2} \right) = 0, \qquad (1.9)$$

resulting in equation for $\tilde{F}^2$

$$\left(\nabla \cdot \frac{\nabla \tilde{F}^2}{r^4} \right) = 0, \qquad \lambda \delta \vec{r} = -\frac{\nabla \tilde{F}^2}{2r^2}, \qquad (1.10)$$

which closes the system and determines the iteration step.

2 VDE of a straight plasma column, CylVDE() routine

Classical case of vertical instability

1. *Cylindrical geometry;*
2. *Straight plasma column with a uniform current;*
3. *Elliptical cross-section*
4. *Quadrupole external field*

1. *Continuous wall (no gaps);*
2. *External equilibrium field is frozen to the wall in advance;*
3. *The wall screens magnetic perturbations from instability*

Wall Touching Vertical Mode (VDE):

1. *Tile surface is transparent to magnetic fields;*
2. *Plasma touching the tiles shortens the gaps*

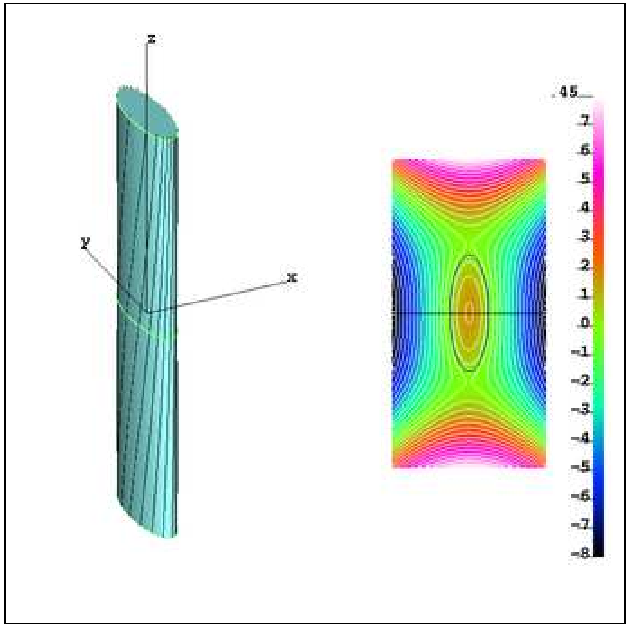

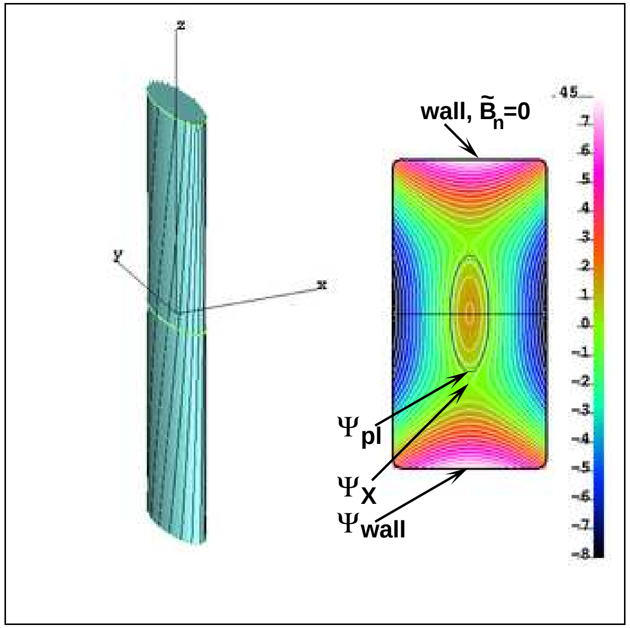

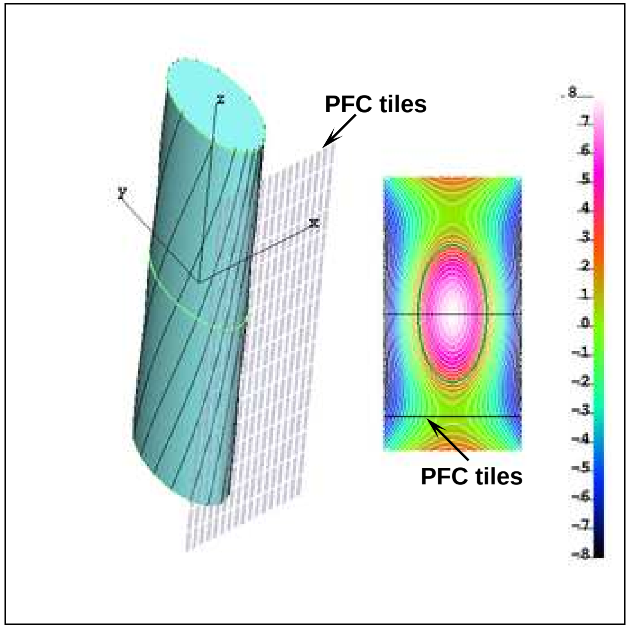

No wall, I_{pl} =const

On left: 3-D plasma geometry and On right: 2-D cross-section. Ψ =const contours are shown in color with a plasma in the center

Ideally conducting wall, $\Delta\Psi|_{core}^{wall}$ =const

Tile surface on the path of the plasma motion.

(In absence and presence of a wall)

Case 0: no wall, no tiles. Nonlinear motion

Generation of surface currents at the plasma boundary due to flux conservation

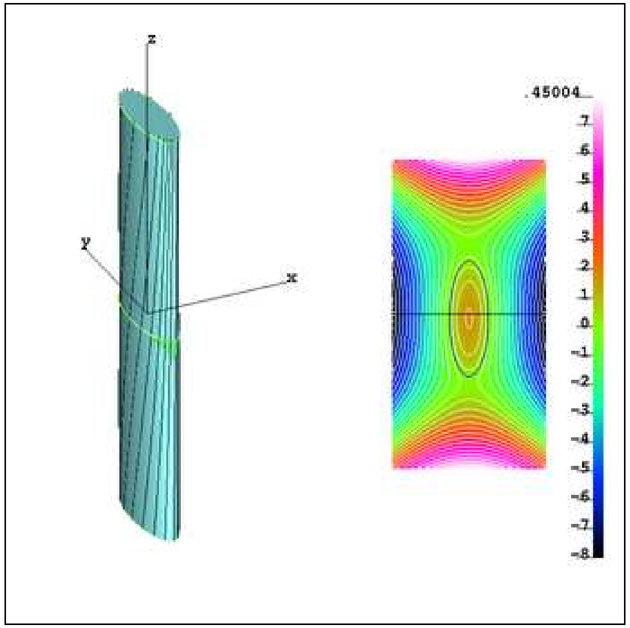

Initial downward plasma displacement

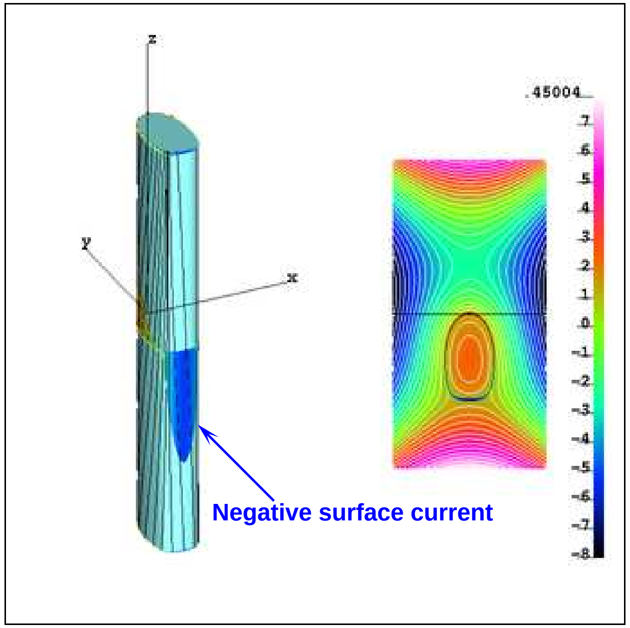

Nonlinear phase of instability. Negative surface current at the leading plasma side

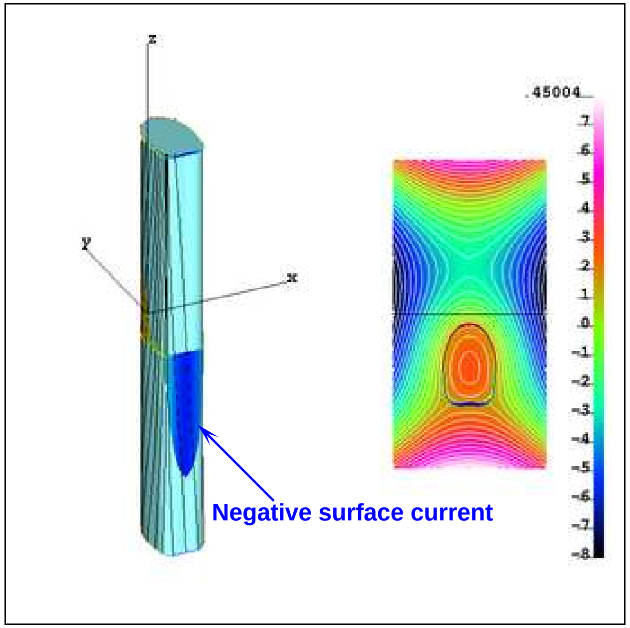

Flattening of the plasma leading side, which faces growing external field

Case 0: Strong external field stops the vertical motion

New geometry for reconnection is discovered: unstable plasma reconnects with a vacuum magnetic field

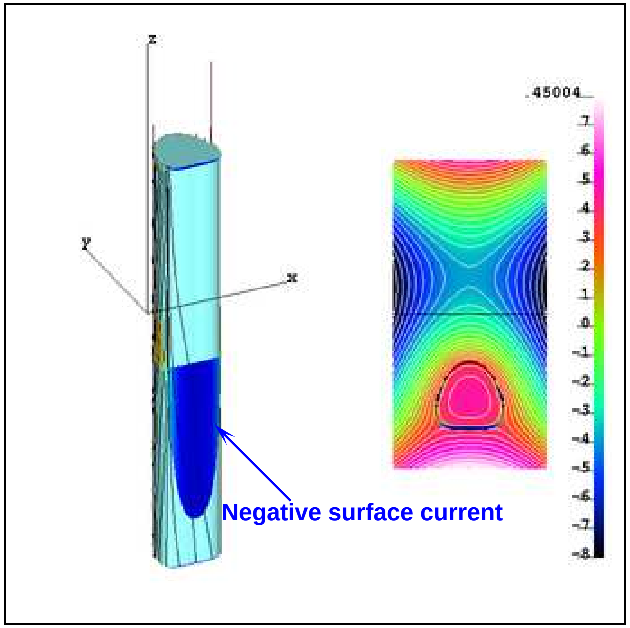

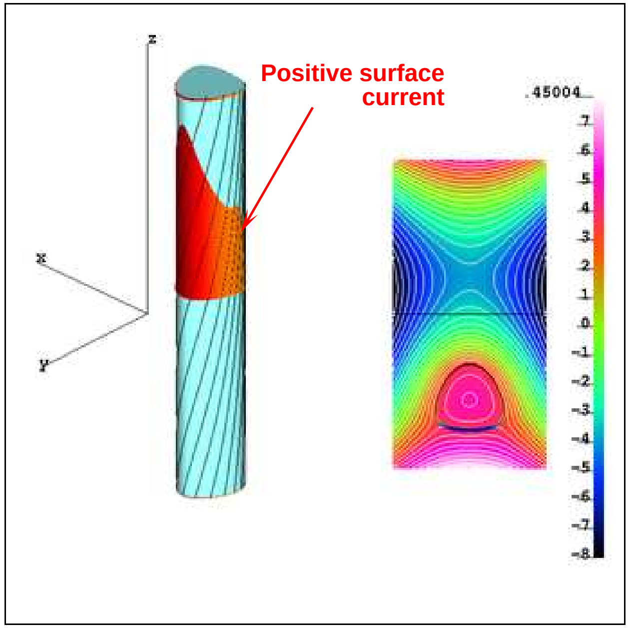

1. ***Strong negative current is generated at the leading plasma edge***
2. ***Plasma cross-section becomes triangle-like***

1. ***Strong positive current is generated at the free plasma edge***
2. ***Plasma stops moving in vertical direction.***

(a) opposite poloidal field $B_\theta^{vac} \simeq -B_\theta^{core}$ across the leading plasma edge;

(b) two Null Y-points of poloidal field in two vertices of plasma cross-section.

Plasma should be leaked through the Y-point untill full disappearance. The simulation of reconnection is beyond the scope of CylVDE().

In the presence of a conducting wall, there are two different situations:

1. $|\Psi_{pl} - \Psi_X| < |\Psi_X - \Psi_{Wall}|$ ***- plasma separated from the wall***
2. $|\Psi_{pl} - \Psi_X| > |\Psi_X - \Psi_{Wall}|$ ***- plasma is close to the wall***

depending on relation between poloidal fluxes at the plasma, in X-point, and at the wall.

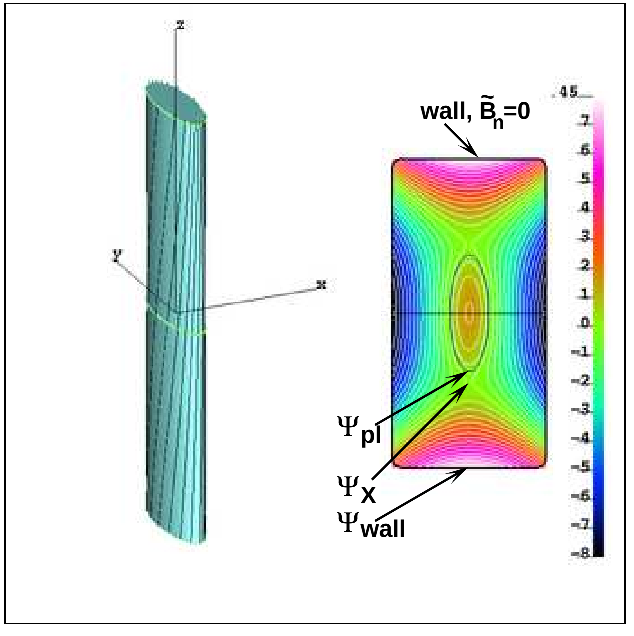

Initial configuration: $|\Psi_{pl} - \Psi_X| < |\Psi_X - \Psi_{Wall}|$

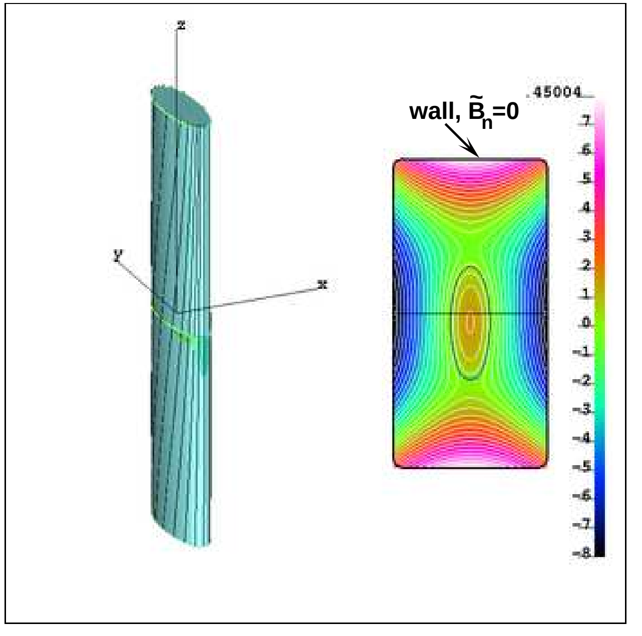

Initial downward plasma displacement

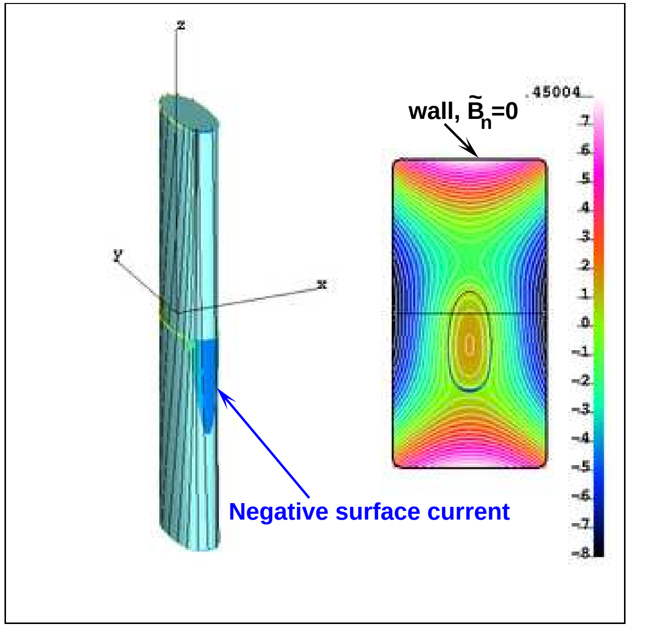

Nonlinear phase of instability. Negative surface current at the leading plasma side

Case 1-a: plasma is separated from the wall

The motion of plasma essentially repeats the instability without wall and finally leads to a reconnection geometry

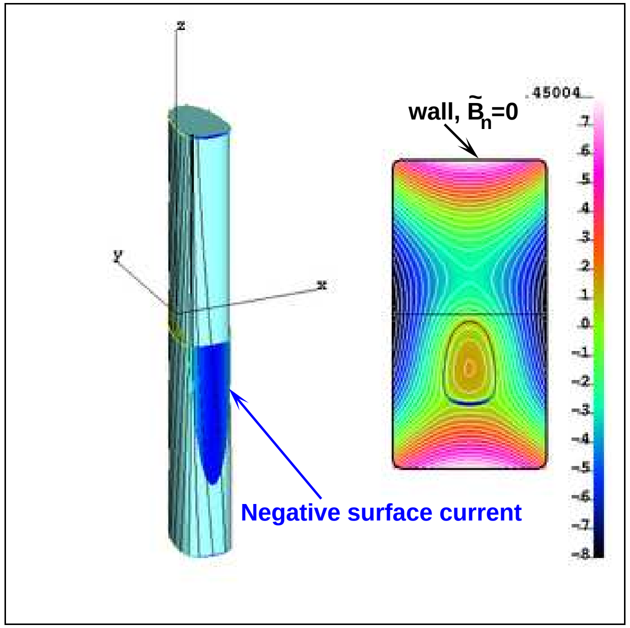

Approaching reconnection geometry with two Y-points at the plasma boundry

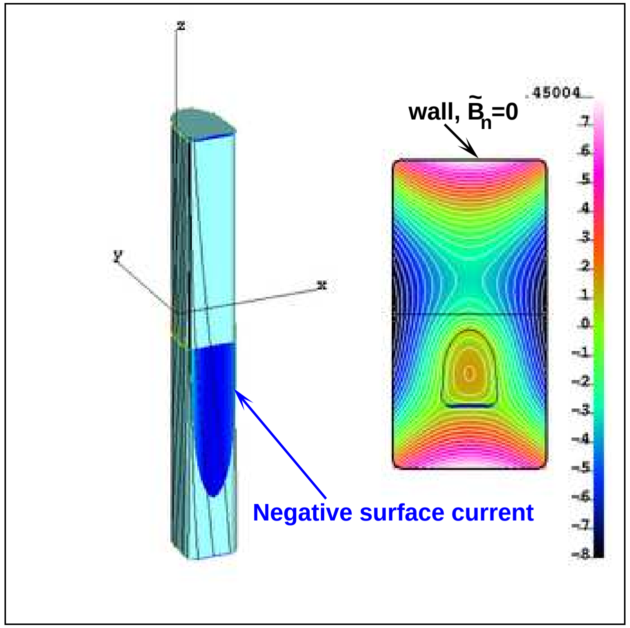

Plasma stops vertically and goes to reconnection

Case 1-b: plasma is close to the wall

Initially, plasma moves as in the previous case.

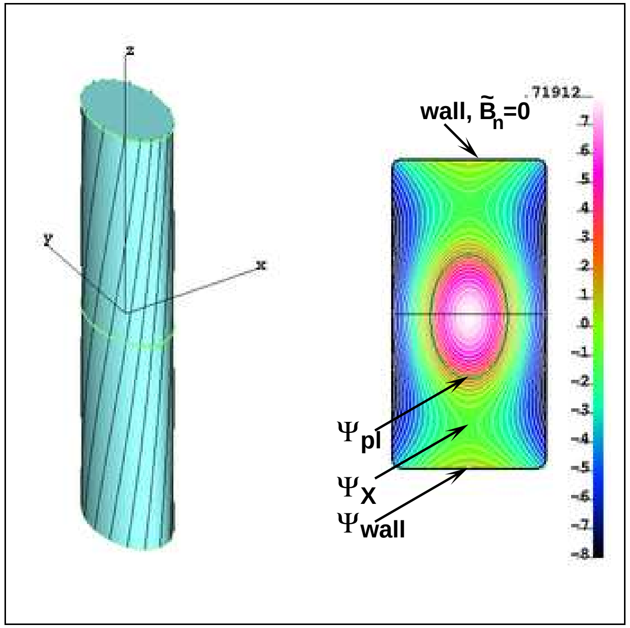

Initial configuration:
$|\Psi_{pl} - \Psi_X| > |\Psi_X - \Psi_{Wall}|$

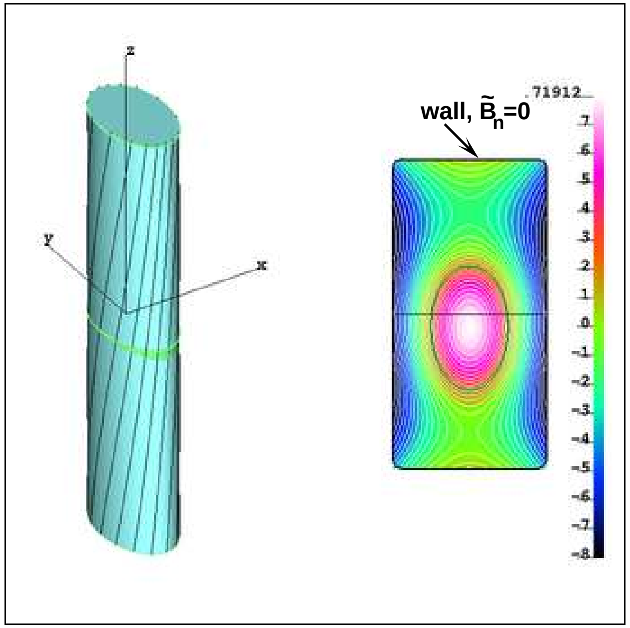

Initial downward plasma displacement

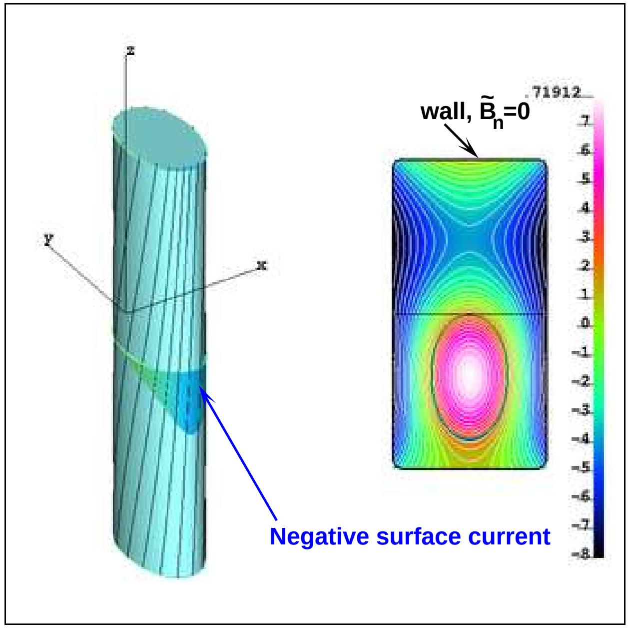

Nonlinear phase of instability. Negative surface current at the leading plasma side

Case 1-b: plasma is close to the wall

Plasma reaches a new equilibrium maintained by the eddy currents in the wall

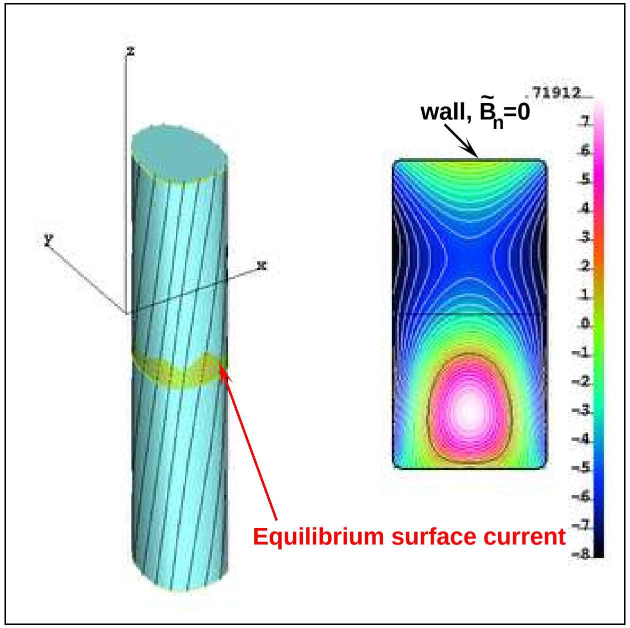

Leading side of the equilibrium plasma. Negative surface current is replaced by a positive one.

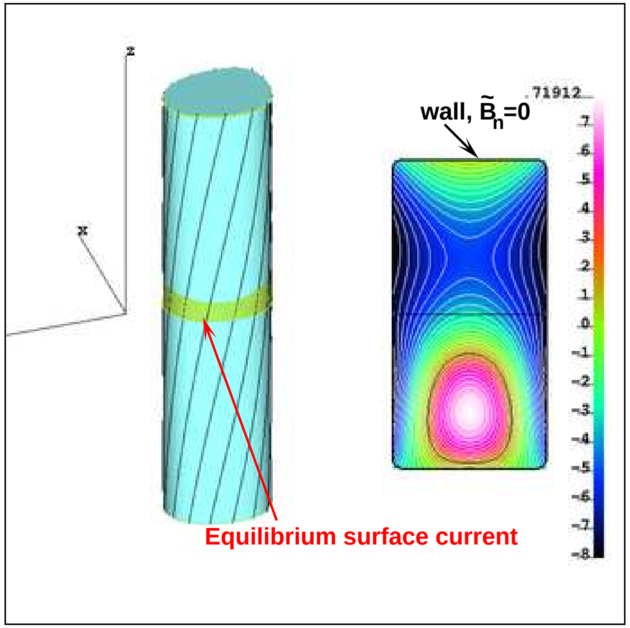

Other side of the equilibrium plasma with a positive surface current.

Tile currents in VDE: original misinterpretation

The physics of VDE was significantly confused in 1991 (Strait et al, Nucl. Fus. 1991) where currents to the tiles were discovered.

The misuse of EFIT reconstruction code led to misinterpretation of these electric currents as "halo" currents.

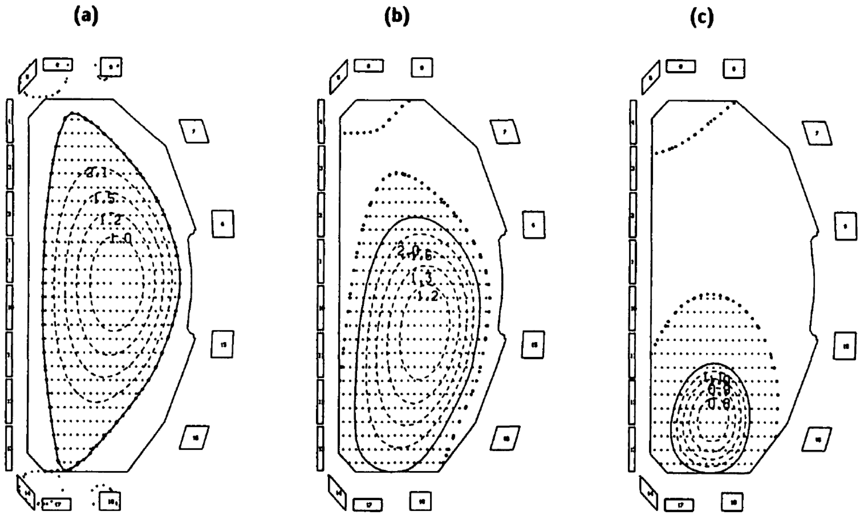

FIG. 3. Equilibrium flux plots from EFIT at three times during the vertical instability: (a) 2660 ms, (b) 2675 ms and (c) 2684 ms. Plasma current was allowed in the hatched region, including part of the SOL.

Figure 1: EFIT reconstruction of plasma configuration in VDE

Despite of wide acceptance by fusion community, the physics picture supporting the halo-current interpretation was never established.

In fact, the model is in strong contradiction witth every direct measurement (JET, EAST).

EFIT equilibrium reconstruction code was designed for the Grad-Shafranov equilibria.

In contrast, VDE is described by TMHD, which includes flux conserved plasma evolution and generation of surface currents.

Case 2: VDE with plasma facing tiles (no wall)

Surface currents at the free flowing plasma are converted to

1. ***Hiro currents affecting the instability, and***
2. ***Evans currents to the tile surface, misinterpreted as "halo" currents***

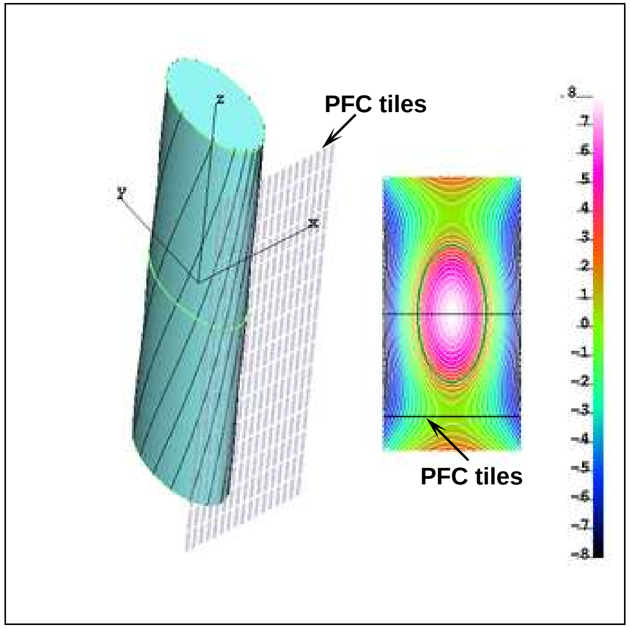

Initial downward plasma displacement

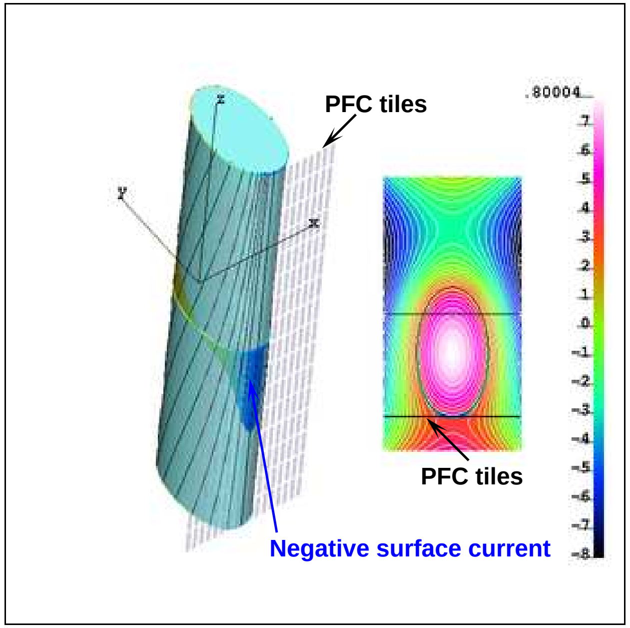

Negative surface current at the leading plasma side

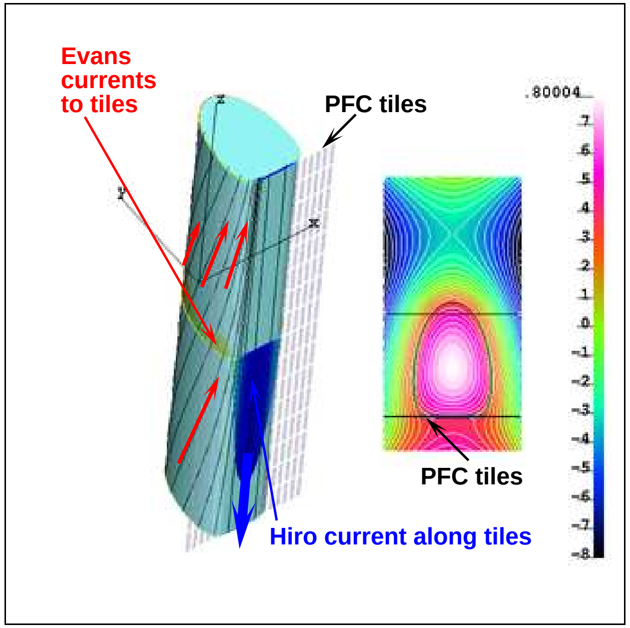

Two distant Y-points are formed at the leading edge

1. ***Negative surface currents are transformed into toroidal Hiro currents***
2. ***Positive surface currents along field lines are partially converted to Evans currents to the tile surface.***

Case 2: VDE with tiles: Evans current (no wall)

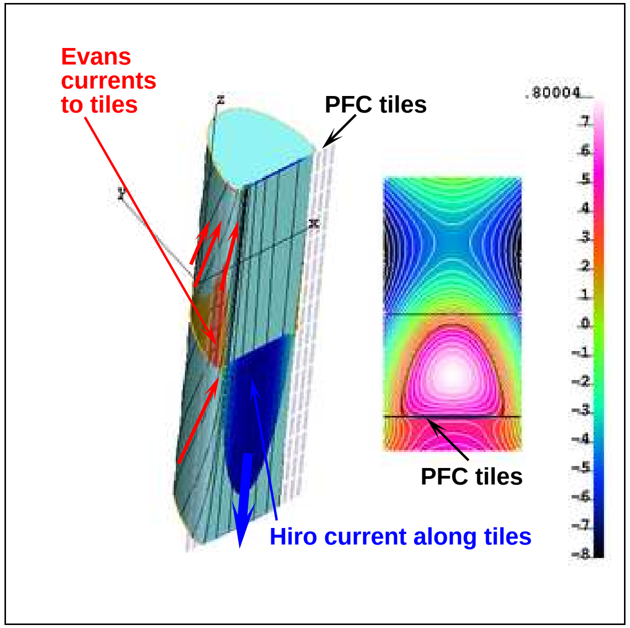

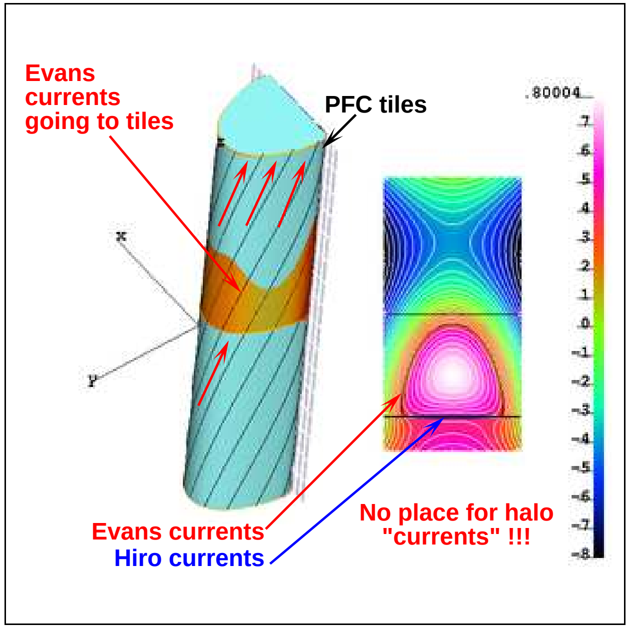

The Hiro currents maintain MHD equilibrium with a force applied to the tiles

Evans currents are the source of tile currents

Two parallel circuits for force-free positive currents:

1. ***with flow to the tiles as Evans currents***
2. ***with flow along the plasma edge***

Evans currents enter the tile surface at Y-points at a distance from the central line.

For the first time, Evans currents give a science based explanation of DIII-D measurements of tile currents

Case 2: VDE with tiles: Shrinking plasma

1. ***Decay of Hiro currents leads to the shrinking of plasma cross-section***
2. ***Two Y-points, which connect the Evans currents with the tiles, remain separated***

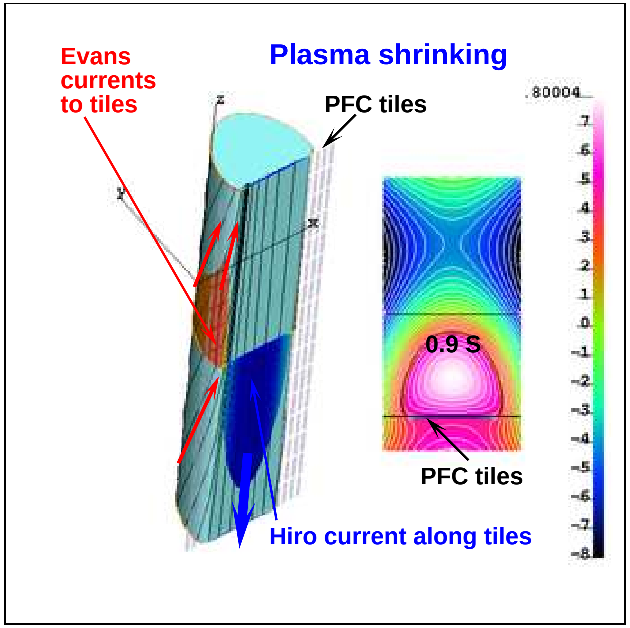

$S = 0.9 S_{initial}$

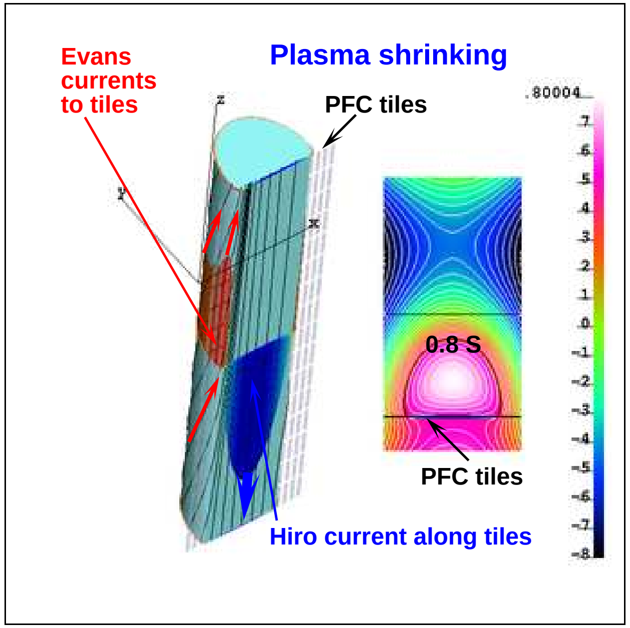

$S = 0.8 S_{initial}$

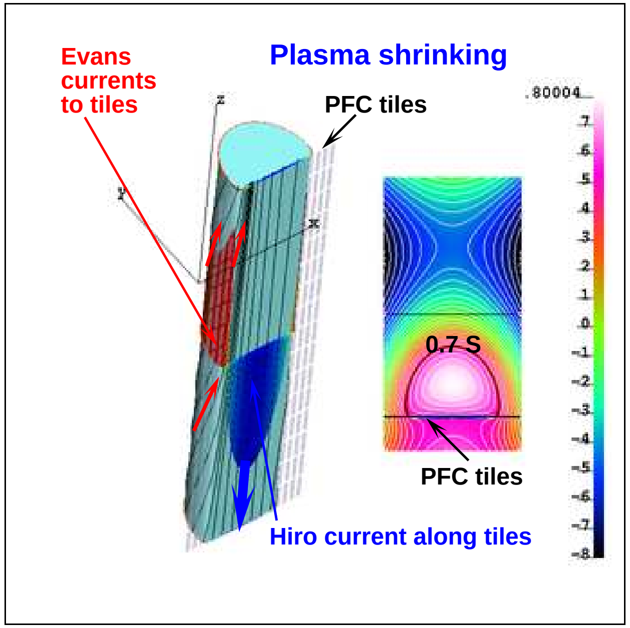

$S = 0.7 S_{initial}$

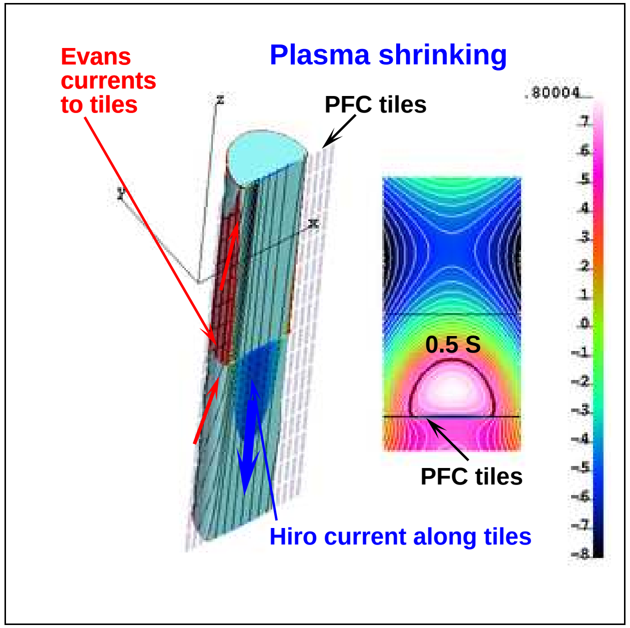

$S = 0.5 S_{initial}$

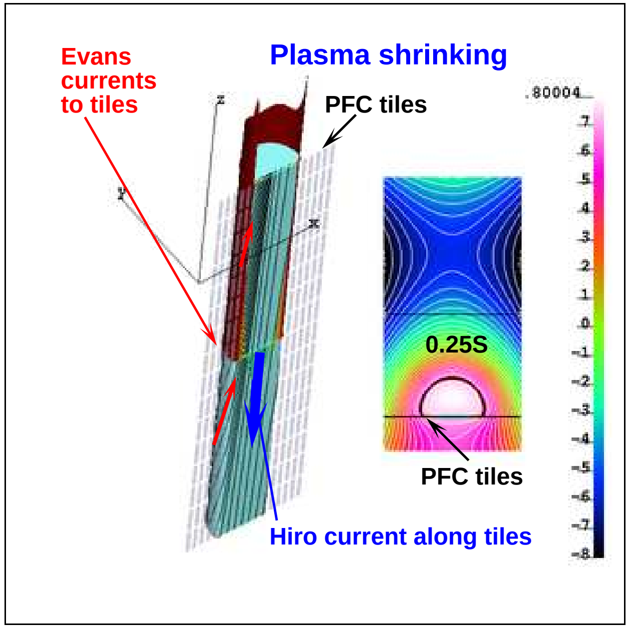

$S = 0.25 S_{initial}$

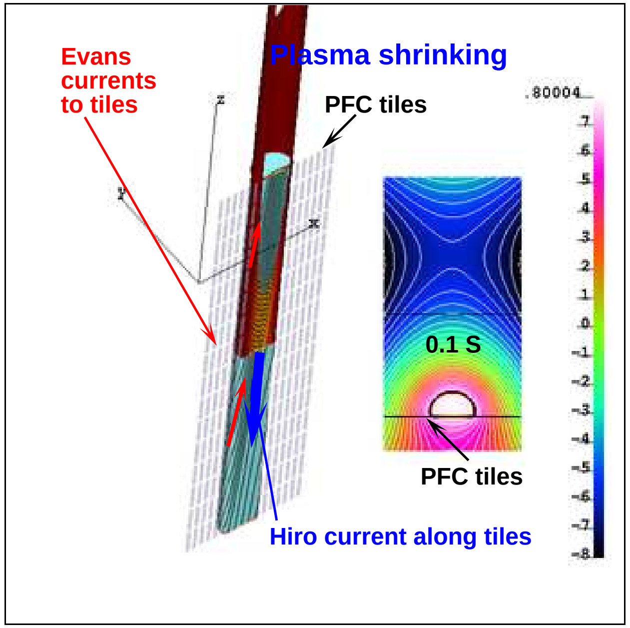

$S = 0.1 S_{initial}$

Y-points remain separated till the end of the plasma

Case 3: VDE with tiles and a wall

In tokamaks, the plasma is always "separated" from the wall based on $\Psi_{pl}, \Psi_X, \Psi_{Wall}$.

The presence of the wall does not affect VDE significantly

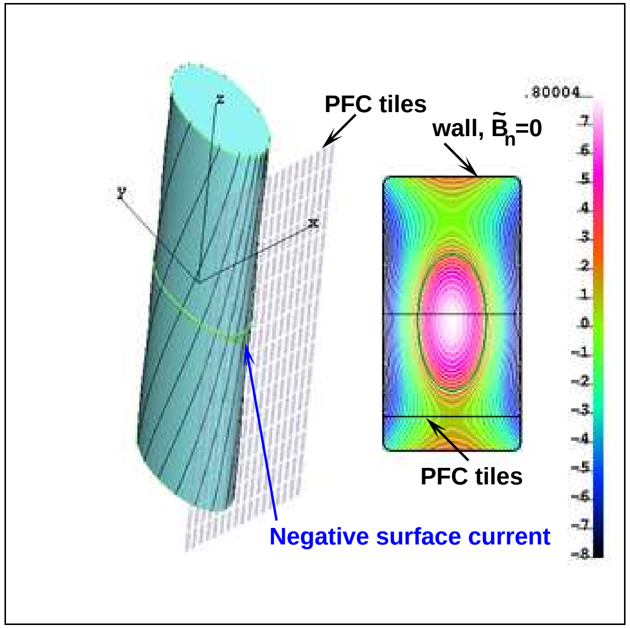

Initial plasma displacement

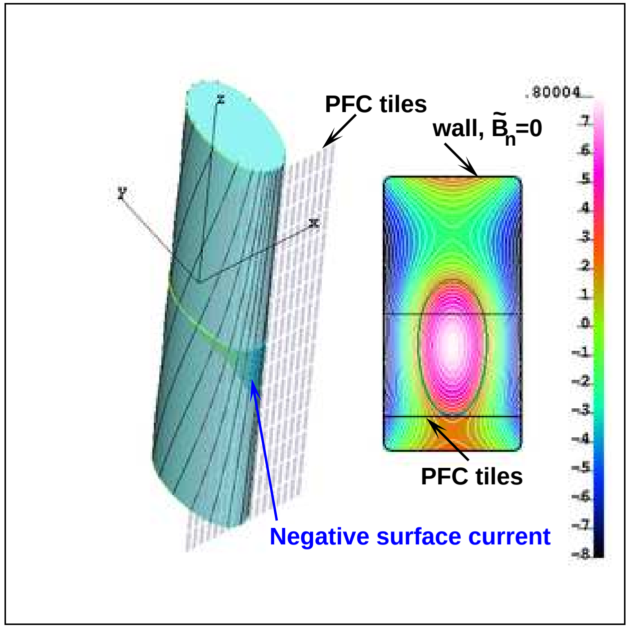

Negative surface current at the leading edge

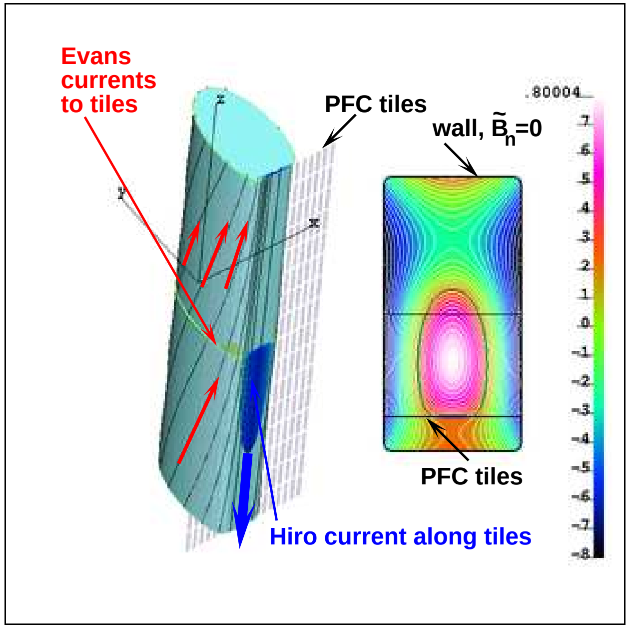

Hiro, Evans currents, formation of two Y-points

Due to stabilizing wall action, Y-points are less separated than in the absence of the wall

Otherwise, the plasma motion in both cases is similar.

Case 3: Intermediate equilibrium (wall and tiles)

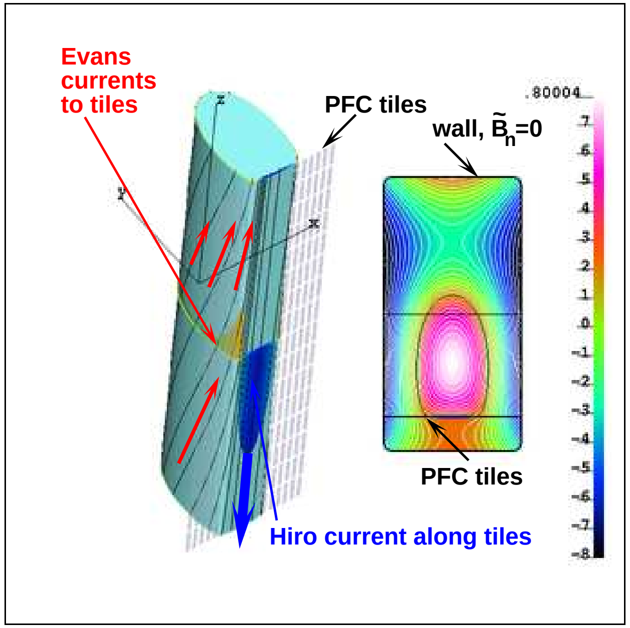

Hiro currents apply the force to tiles

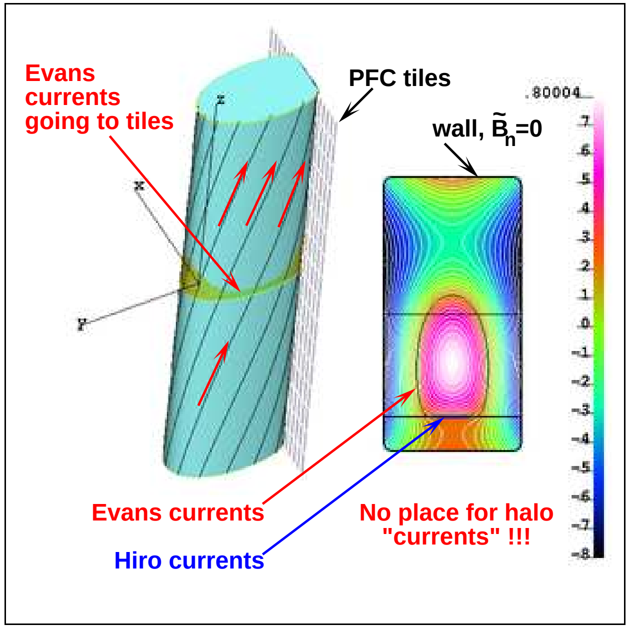

Evans currents. No place for fake "halo" currents

Case 3: Plasma shrinking (wall and tiles)

Plasma shrinking due to decay of Hiro currents

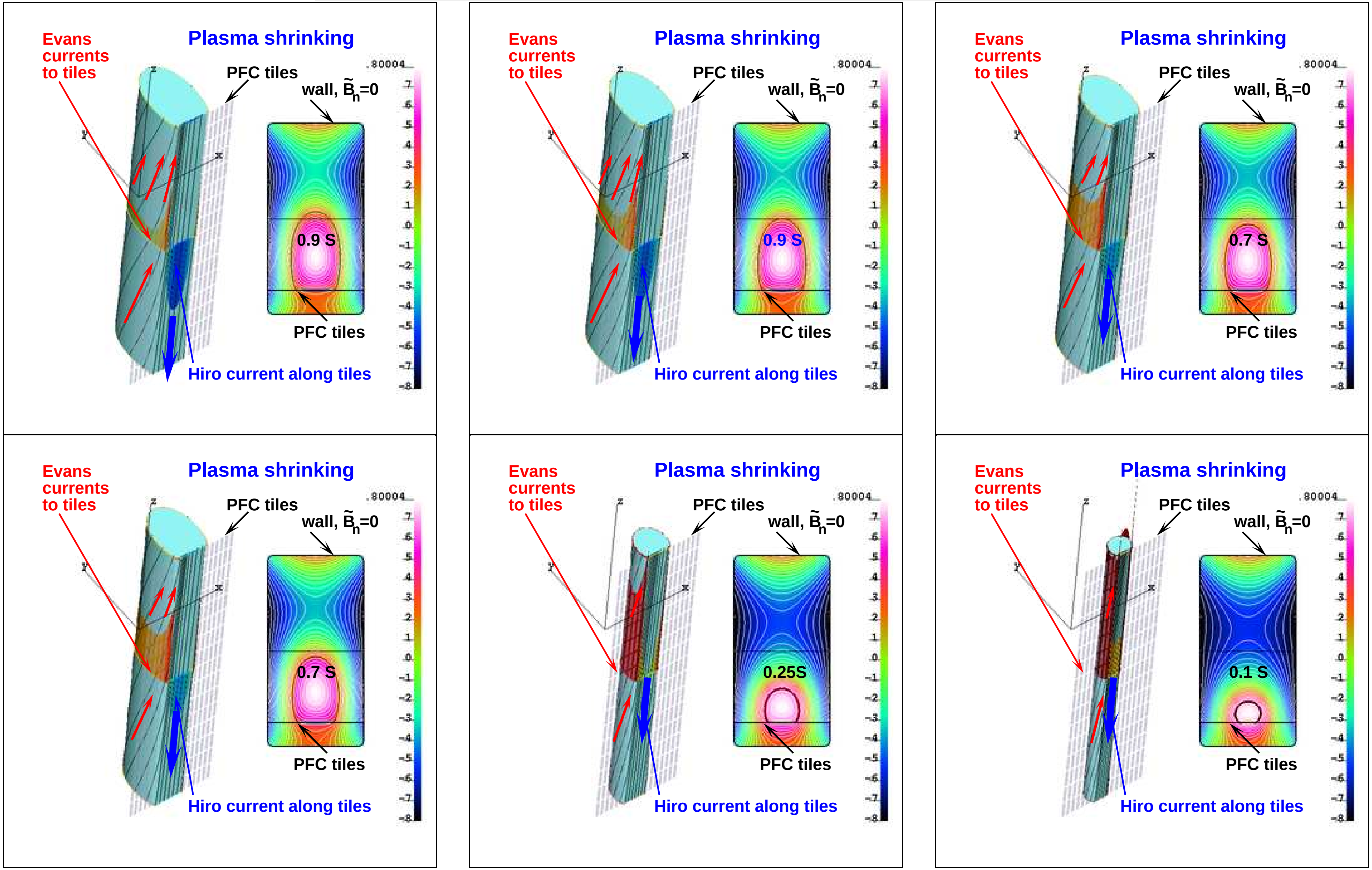

3 VDE on EAST

Xiong tiles on EAST - New diagnostics for VDE

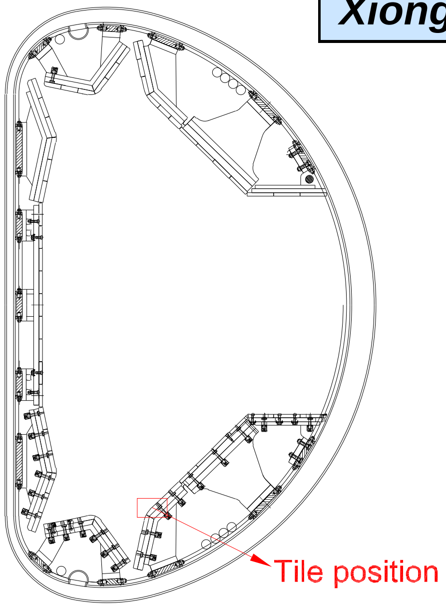

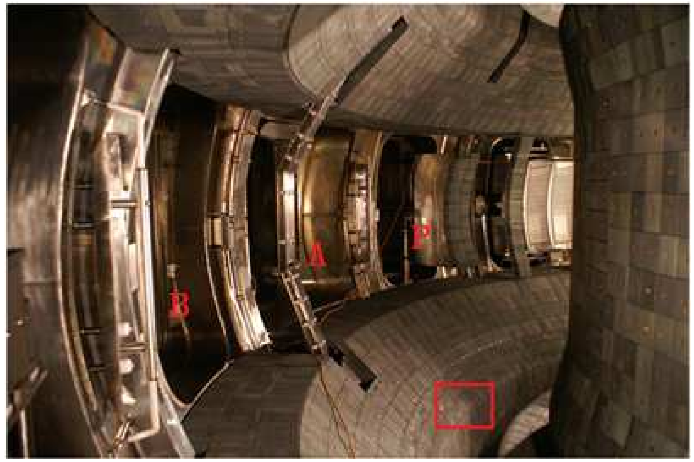

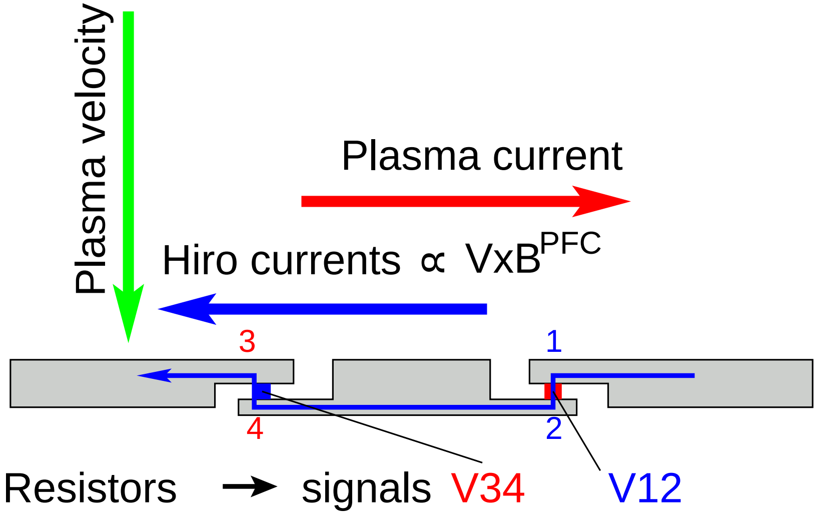

4 types of currents can be distinguished by Xiong tiles.

First measurements of Hiro currents in VDE

Xiong tile diagnostics on EAST in May 2012 unambiguously confirmed generation of negative Hiro currents in toroidal direction

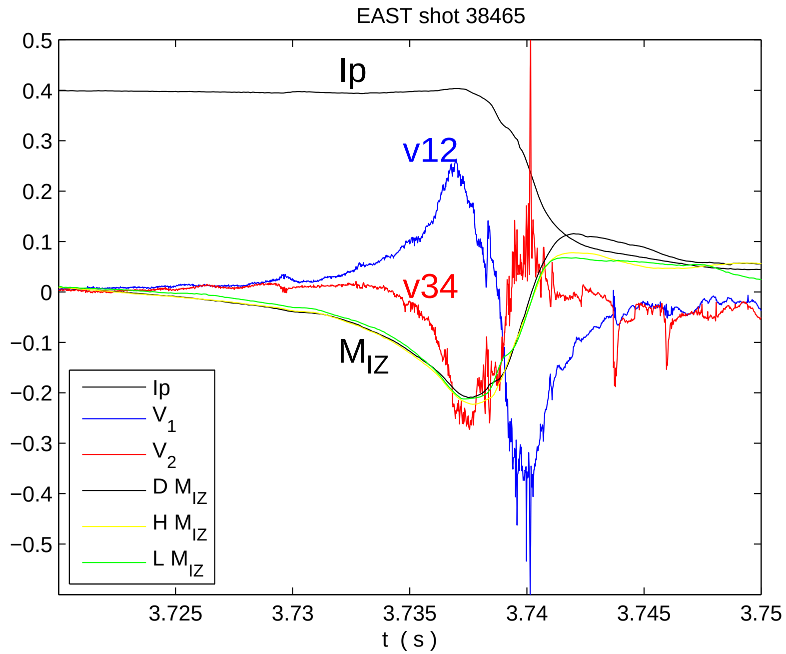

Downward VDE

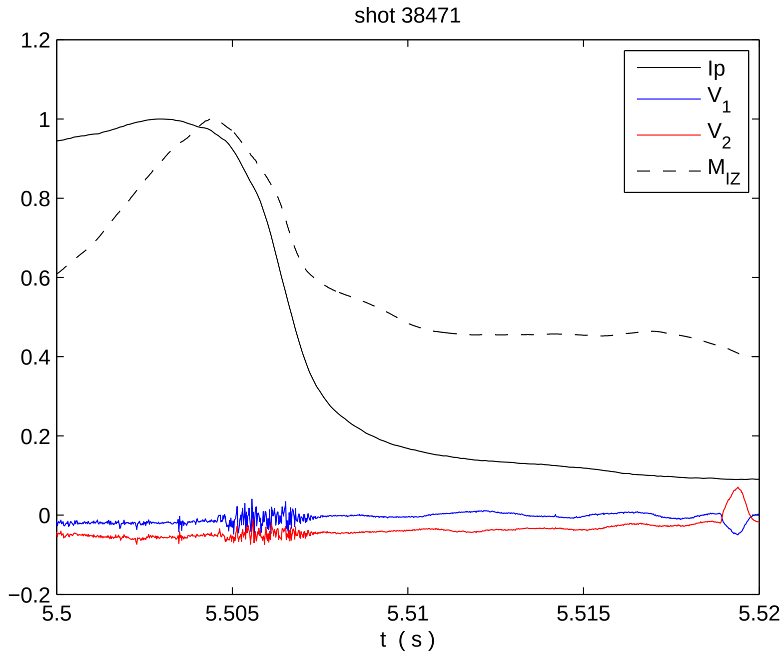

Upward VDE

No toroidal asymmetry.

Hiro currents in VDE are NOT EXCHANGED between plasma and the tiles.

EAST is the next device after JET and COMPASS in high quality of magnetic diagnostics. We are preparing our VDE code to simulate EAST measurements.

4 Vacuum chamber in EAST

Real EAST in-vessel geometry is used for VDE simulations.

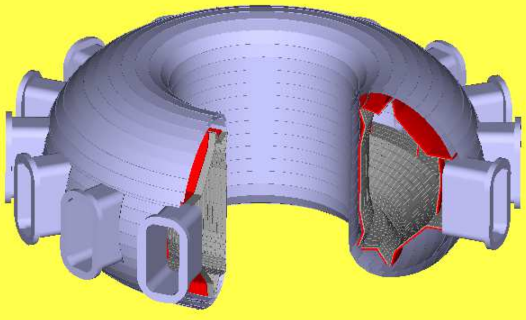

Vacuum Chamber

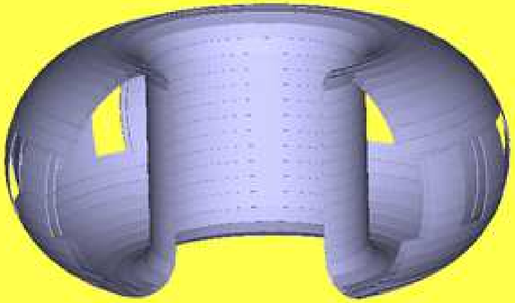

Double layer vacuum vessel

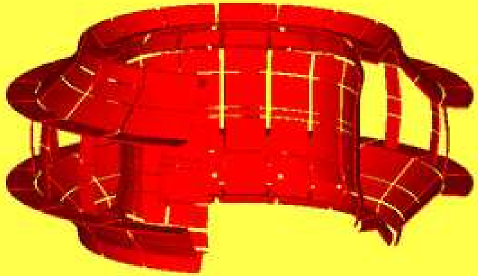

Stabilizer elements (16 toroidal sections)

One toroidal sector of copper stabilizers (8728 triangles)

Numerical model of EAST passive structures (as of 2008)

2014 update is available, but not yet implemented

Carbon plasma facing tiles

5 TorVDE() for VDE simulations on EAST

Real EAST in-vessel geometry is used for VDE simulations.

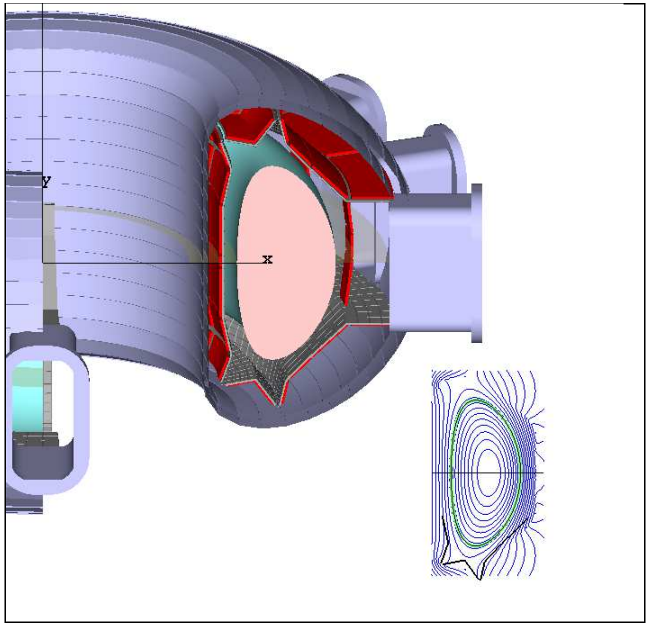

Initial unstable plasma

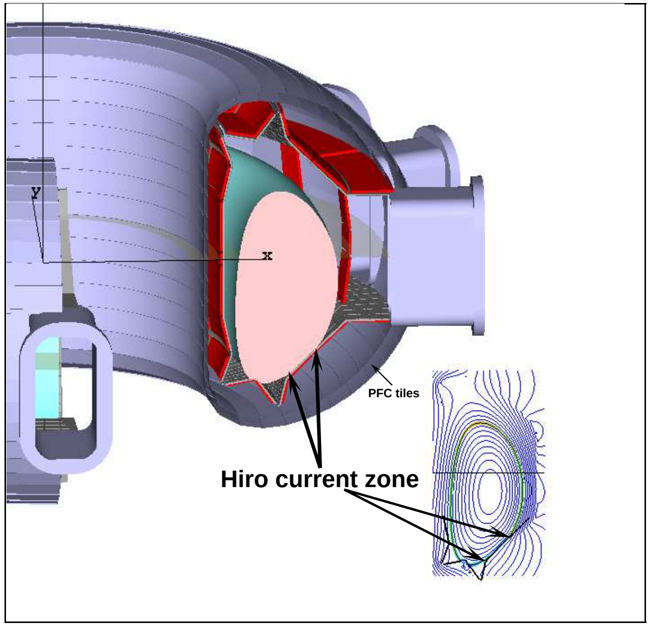

Plasma touches the divertor plate and generate Hiro currents, $\Phi/\Phi_0 = 1$

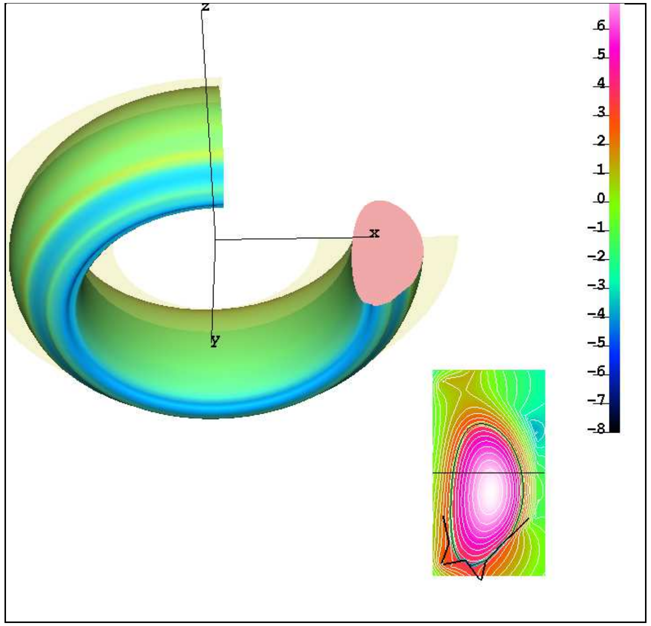

Negative Hiro currents (blue), shown in the contact area of plasma

!!! Our VDE code shows the contact zone right at the position of Xiong tiles !!!

Plasma VDE in EAST geometry

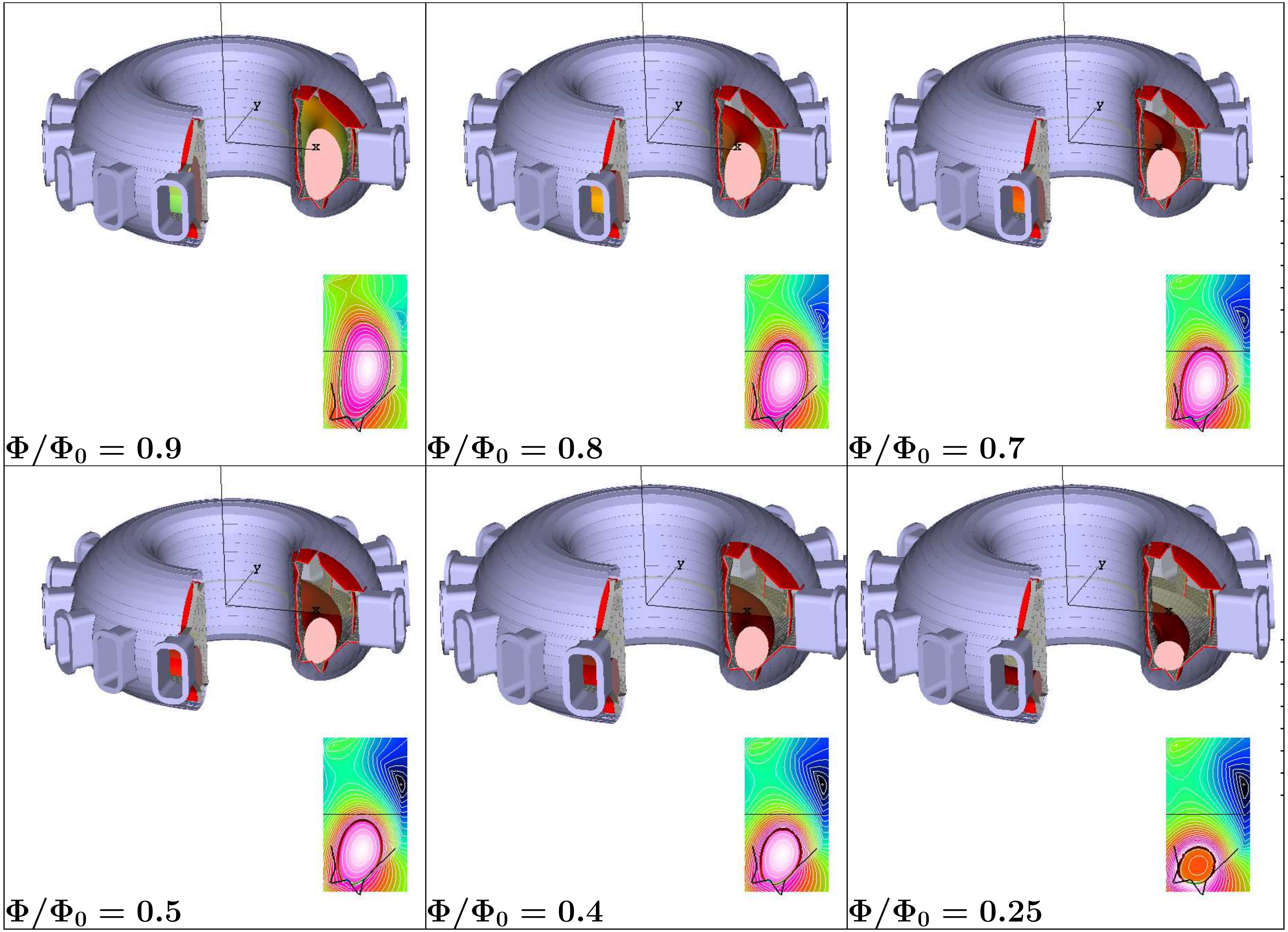

We suggested a comprehensive set of innovative tile diagnostics for Hiro, Evans and SoL current measurements on NSTX-U

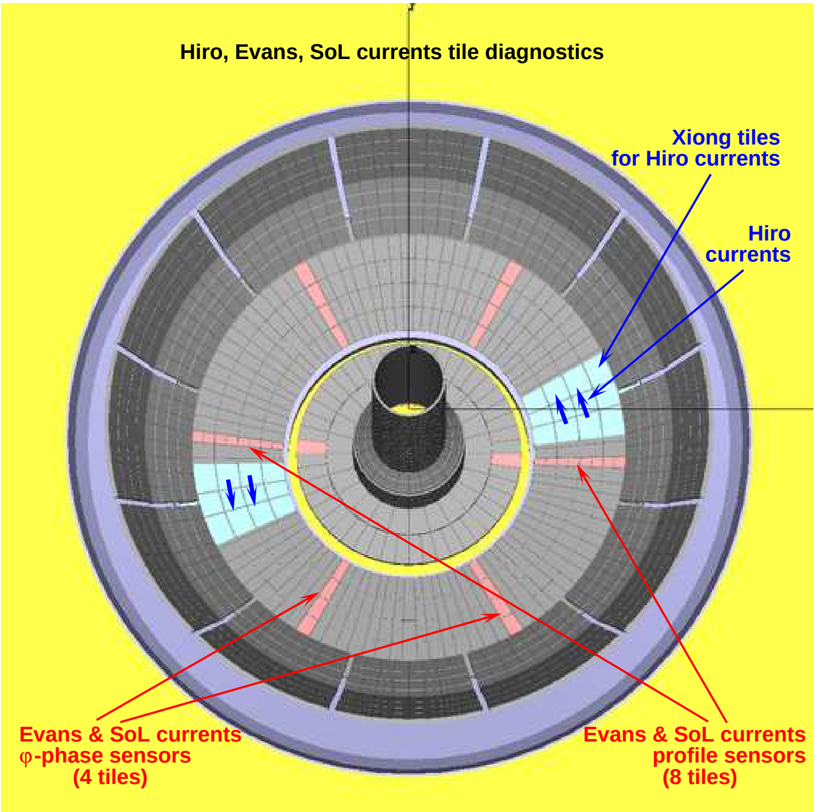

Tile sensors for measuring Hiro, Evans, and SoL currents and different kinds of diagnostics including

1. ***Hiro current diagnostics***
2. ***Evans current profile diagnostics with enhanced radial resolution***
3. ***Evans current φ-phase diagnostics***
4. ***SoL current measurements***

Evans currents carry important information on plasma-PFC interactions, never touched

7 Summary

- ***VDE code* were created in short time to address urgent needs in VDE simulations.**
- ***Its keywords:* TMHD model, adaptive grids, generation of Hiro and Evans currents, five distinct regimes for VDE.**
- ***Reconnection of plasma and vacuum field* is discovered as a new plasma physics effect**

For the first time, the scientific explanation of the tile current measurements in VDE is developed:
Evans currents, generated by instability, are, in fact, what is measured in tokamaks

- ***The Hiro currents* create an intermediate plasma equilibrium. Hiro currents are responsible for the force to the structure.**
- ***Evans currents* are force-free. They are a fraction of the positive surface currents which is limited by the ion saturation current. The rest of it is closed through the plasma edge.**

Hiro and localized radially Evans currents carry unique information on plasma-wall interaction.
We proposed an innovative tile diagnostics in order to reveal this important information

Our VDE code is a tool giving confidence in possibility of realistic modeling of tokamak VDE and plasma.